Polarized Light Scattering and its Application to Microroughness, Particle, and Defect Detection

Thomas A. Germer

Optical Technology Division
National Institute of Standards and Technology
Gaithersburg, MD 20899

In this paper, I will discuss the theory and application of polarized light scatter. Recent measurements have shown that some sources of scatter, including microroughness and subsurface defects, have well-defined polarizations for any specific pair of incident-scatter directions. By exploiting this knowledge, polarization techniques offer the possibility for large improvements in the sensitivity to defects and the discrimination of those defects from competing sources of scatter. The theoretical performance of a specific polarized light scattering instrument configuration will be analyzed to illustrate that a factor of 1.4 improvement in the minimum detectable particle or defect size can be readily attained.

INTRODUCTION

Optical scattering techniques have proven to be very useful for the detection of defects on silicon wafers in the ramp-up and high-yield stages of production. Since detectors for optical radiation can be extremely sensitive and fast, and since optical techniques lack vacuum requirements and, in many cases, stringent vibration tolerances, the techniques are ideal for tools with the high throughputs required for these stages of production. However, these techniques will inevitably run into barriers as feature sizes continue to be reduced. The particle sizes that will need to be detected are much smaller than the wavelength of the light used for the measurement, where the scattering cross section decreases rapidly. Therefore, small decreases in feature size translate into large increases required in the detection sensitivity. Furthermore, sources of delocalized scatter, such as microroughness, can dominate the signal, especially on blanket layers.

Since the scattered light intensity is affected by laser speckle noise, it is difficult to imagine that instruments relying upon the intensity alone will meet the new demands on optical inspection techniques. Since roughness, as spatial noise, has an associated randomness, fluctuations in the measured scattered light intensity prohibit detection of the smallest particles. Furthermore, since real-life particles are not perfect spheres, the directional distribution of light scattered by them will not necessarily replicate that of perfect spheres. Lastly, given the number of different types of defects that exist on wafers, an instrument designed with a small number of light collection directions that are optimized to enhance sensitivity to one class of defect in comparison to another will lack the discrimination capabilities to tell them all apart.

The polarization of scattered light can often yield significant information about the source of that scattered light[1,2]. Recent measurements have demonstrated that the light scattered by microroughness has a well-defined polarization that is independent of the microscopic details of the roughness[3]. Furthermore, other scattering sources, such as particles above the surface or defects below the surface give rise to polarizations that differ from those predicted by microroughness.

By using polarization-sensitive detectors, a system can be built which is insensitive to a particular scattering source[4]. Since these scattering sources yield well-defined polarizations in all scattering directions, the question of what optical geometry is most sensitive to different types of defects becomes moot since light over the entire scattering hemisphere can be utilized.

In this paper, I review the theory of polarized light scatter and present data and theoretical predictions to demonstrate the validity of the models and to illustrate the behavior of those theories. A specific design for a microroughness-blind instrument is presented, and the improvements in particle and defect detection limits are calculated.

THEORY

Theories for scattering from particulate contaminants and subsurface defects in the Rayleigh approximation and from microtopography have been developed elsewhere[1,5,6]. Each of these theories predicts a closed form expression for the Jones scattering matrix,

$$\begin{pmatrix} S_{ss} & S_{ps} \\ S_{sp} & S_{pp} \end{pmatrix} \tag{1}$$

which relates the scattered electric field to the incident electric field. The p and s linear polarization states are defined such that the electric field is parallel and perpendicular, respectively, to the plane defined by the surface normal and the direction of propagation.

Within the Rayleigh approximation, where the size of the scatterer is much smaller than the wavelength of the light, a scatterer may be treated as a point polarizable dipole. The induced dipole moment is proportional to the local electric field, and it radiates locally in each direction with an amplitude and polarization determined by the projection of the dipole moment onto the plane perpendicular to the direction of propagation. The propagation of light to a detector must include the relevant reflections and

Published in "Characterization and Metrology for ULSI Technology," edited by D. G. Seiler, W. M. Bullis, A. C. Diebold, R. McDonald, and T. Shaffner (American Institute of Physics, New York, 1998), pp. 815-818

refractions that occur at each surface. Using this approximation, the polarization of light scattered by a particle above a surface, a defect below a surface, or a defect within a dielectric layer can be readily calculated[1,7].

The light scattered by small degrees of roughness has been calculated for a single interface[5], or by one or more interfaces in a stack of dielectric layers[6], using first-order vector perturbation theory. The solution to the roughness problem can be shown to be similar to that for defects with a small difference: the light scattered by the roughness of a particular interface is equivalent to dipoles generated by the electric field above that interface, which then radiate from below the interface (or vice versa)[8]. The polarization of the light scattered by a single microrough interface into a specific direction is only a function of the optical constant of the material and not of the power spectrum of the roughness. When the roughness of multiple interfaces contribute to scattered light, then the polarization also depends upon the correlation functions of the roughness between the different interfaces.

For scattering in the presence of a single interface, the largest contrast between particles, defects, and microroughness occurs when p-polarized light is incident on the sample at an oblique angle. In this case, the electric field inside the material has a different direction than that immediately outside the material. That is, for a high index material, such as silicon, the electric field just outside of the material is nearly perpendicular to the surface, while the electric field inside the material is nearly parallel to the surface. A detector viewing the polarization out of the plane of incidence effectively observes the direction of the dipole moment induced in the defect. For s-polarized incident light, the electric field direction does not depend upon location, resulting in a lack of sensitivity of the scattered light polarization to the location of the defect.

EXPERIMENT

Measurements of the polarization of light scattered by a sample given a fixed incident polarization, herein referred as bidirectional ellipsometry, have been measured using a goniometric optical scatter instrument[9]. Continuous wave p-polarized light of wavelength λ is allowed to be incident upon each sample at an angle θ_i. Light scattered into a polar angle θ_s and azimuthal angle ϕ_s (defined with respect to the plane of incidence) is collected with a polarization-analyzing detector. The results are presented in terms of a principle angle of polarization, η, and a degree of linear polarization, P_L, as functions of ϕ_s for fixed θ_i and θ_s. The angle η is measured with respect to s-polarization in a counterclockwise fashion looking into the beam. The parameter P_L lies in the range $0 \le P_L \le 1$, with $P_L = 1$ indicating linearly polarized light, and $P_L = 0$ indicating either circularly polarized light, or completely depolarized light.

The uncertainties in P_L tend to be dominated by random sources, including electronic noise and laser speckle. When $P_L = 1$, the value of η has a typical uncertainty determined by electronic noise and the alignment and quality of the optical elements. Although a complete discussion of these uncertainties is beyond the scope of this paper, the expanded uncertainties (with a coverage factor of $k = 2$) of η and P_L are not expected to exceed 5° and 0.05, respectively[9].

RESULTS AND DISCUSSION

Figure 1 shows bidirectional ellipsometry results for four silicon samples at 532 nm: two photolithographically generated microroughness standards (R1 and R2), the rough backside of a silicon wafer (R3), and a wafer exhibiting a high density of crystal originated particles (COP). The three rough samples (R1, R2, and R3) each scatter light at large angles by amounts differing by about two orders of magnitude from the next. The values of η for the rough samples agree very well with the microroughness model. That this agreement is so good even for the silicon wafer backside is surprising since the small-amplitude assumptions of the model are violated.

The polarization of the light scattered by the COP sample deviates from that of the microrough samples to a significant degree. In fact, the data seem to lie much closer to the subsurface defect model, in agreement with the current understanding that COPs are coalesced vacancies below the surface[10]. That there exist deviations of η from the subsurface defect model indicates that the model is incomplete, perhaps because the finite sizes and shapes of the defects have not been accounted for, or because a second source of scatter is interfering with the measurement.

The theory for scattering due to microroughness predicts the degree of linear polarization to be $P_L = 1$ for all of the

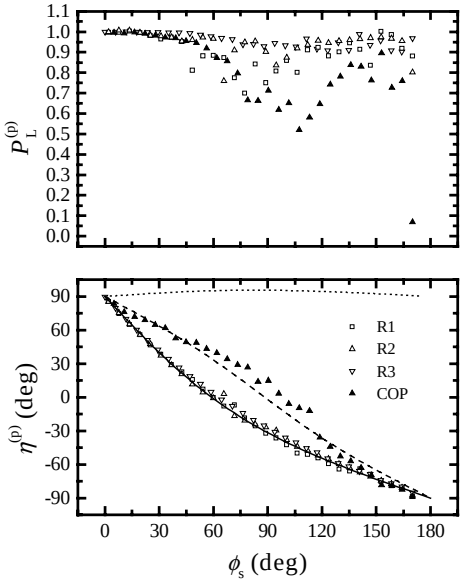

FIGURE 1 Bidirectional ellipsometry parameters for four different silicon samples for p-polarized incident light. The incident and scattering polar angles were $\theta_i = \theta_s = 45°$. The curves in the lower frame represent the predictions of the microroughness (solid), subsurface defect (dashed), and particle (dotted) models.

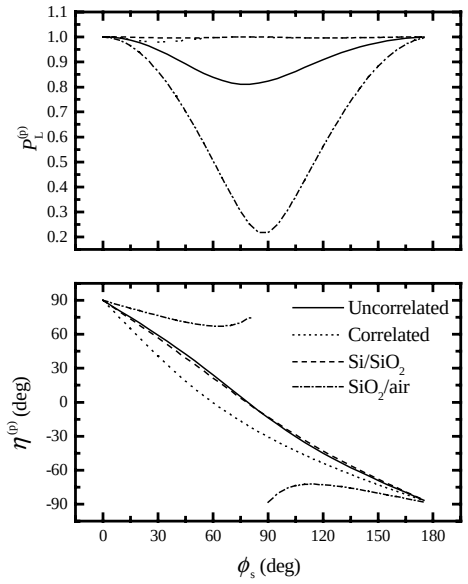

FIGURE 2 Predicted bidirectional ellipsometry parameters for scattering of p-polarized light from microroughness of a silicon wafer with a 5 nm thick oxide.

directions shown in Fig. 1. The data shows reasonable agreement with this prediction for most of the rough samples shown in Fig. 1, where most of the data has $P_L > 0.9$. The lowest scatter sample has randomly deviating data for directions near $\phi_s = 90°$, which may be an artifact associated with the low signals and scatter elsewhere in the laboratory. The values of P_L for the COP sample has a marked deviation from unity for directions $\phi_s > 90°$.

The particle scattering model, which is also shown in Fig. 1, yields a significantly different behavior from those of microroughness and subsurface defects. Since the electric field close to, but outside of, the surface is nearly perpendicular to the surface, the light is expected to scatter with nearly p-polarization ($\eta \sim 90°$).

The scattering from roughness in the presence of a dielectric layer becomes more complex due to the interference between the two interfaces. When more than one interface is rough, then one has effectively multiple sources of scatter. These sources can scatter coherently or incoherently, depending upon the correlation between the roughness of the interfaces. Figure 2 shows the effect that a 5 nm oxide layer can have on the bidirectional ellipsometry parameters. Shown are calculations for roughness from each interface alone and for correlated and uncorrelated roughness. There is a possibility that some of the measured deviations of P_L from unity observed for the microrough sample in Fig. 1 result from the existence of an uncorrelated native oxide.

NEW TOOLS

The finding that microroughness gives rise to scattering with a high degree of polarization in every direction, different from that of other scattering mechanisms, suggests that tools can be developed which are effectively

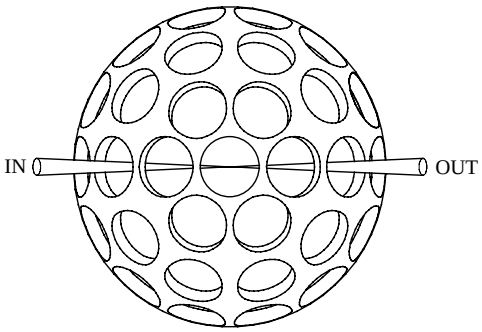

FIGURE 3 Example optical scatter instrument having twenty eight ports, each with a lens, polarizer, and a detector. Three extra ports are provided for the incident beam, the specular beam, and for support.

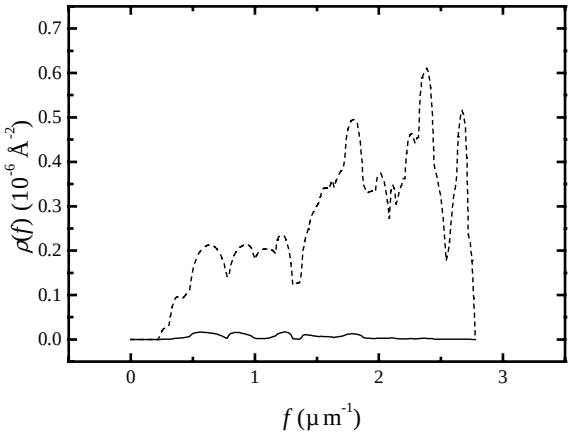

FIGURE 4 The microroughness response function for the instrument shown in Fig. 3. The solid line represents the response function for the system having polarizers aligned in a microroughness-blind configuration. The dashed line represents the response of the system when it does not have the polarization sensitive elements. The light has wavelength 633 nm, and is incident at an angle of 49° with p-polarization.

blind to microroughness[4] These tools do not need to operate under the assumption that a specific detector position is ideal for a specific type of defect. In fact, light scattered into every direction can be collected and discriminated, allowing the elimination of specific scattering sources from the signal, without seriously sacrificing sensitivity to other defects.

Such an instrument is illustrated in Fig. 3. A hemispherical shell contains 31 ports, with central polar angles of 0°, 24°, 49°, and 74°, each spanning a half-angle of 9.5°. Three ports are dedicated to the incident beam, the specular beam, and mechanical support (normal). Each of the other 28 ports holds a collection system with a lens, a polarizer, and a detector. All of the signals are assumed to be summed in this discussion. In this section, I will analyze the predicted performance of this system with and without polarizers.

A methodology has been developed to describe the sensitivity of an optical scatter instrument to micro-

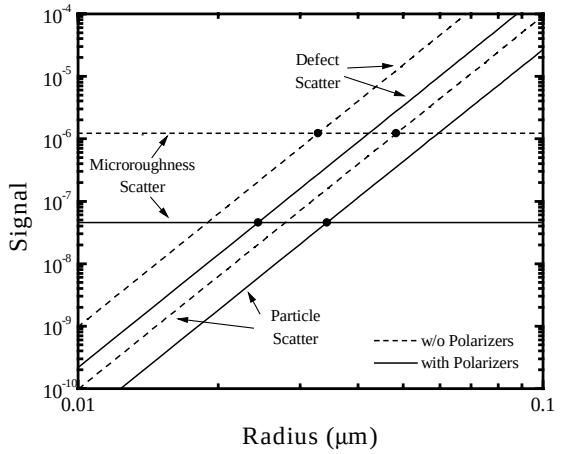

FIGURE 5 The calculated signal for particles as a function of radius for the system shown in Fig. 3 with and without polarization-sensitive detection. The horizontal lines correspond to the microroughness-induced scatter. The intersections of the microroughness/particle scattering functions are marked, indicating the decrease in particle size that can be detected with polarization-sensitive detection.

roughness[11]. A response function, $\rho(f)$, can be defined, so that the roughness-induced signal measured by an optical scatter instrument, *H*, is

$$H = \int_0^\infty df \; 2\pi f \; \rho(f)\, S(f), \qquad (2)$$

where $S(f)$ is the two-dimensional power spectral density (PSD) function of the surface height function. Figure 4 shows the function $\rho(f)$ for the scatter instrument illustrated in Fig. 3, with and without polarizers aligned to reduce microroughness-induced signal. Since each detector collects light over a finite solid angle, and thus the polarizer is only optimized for the center of the aperture, the extinction of microroughness-induced signal is not perfect.

It is possible to make an estimate of the minimum detectable particle size assuming the models for microroughness-induced and particle-induced scatter. For this calculation I will make an assumption that a typical roughness PSD function is given by

$$S(f) = 0.4\,(f \times \mu\text{m})^{-2.5}\,\text{Å}^2 \quad \mu\text{m}^2. \qquad (3)$$

The fractional standard deviation of the noise associated with laser speckle can be estimated to be

$$\sigma_H / H = (\Delta x\, \Delta f)^{-1/2} \approx 0.2, \qquad (4)$$

where Δx is the laser spot size and Δf is the instrument bandwidth from Fig. 4. The detection level for particles or defects is typically set about 5 times the standard deviation of the background noise to maintain the false count rate at a negligible level. Figure 5 shows the results of these calculations. I have assumed that the particle has an index of refraction of $n = 1.5$, a defect has an index of refraction of $n = 1$, and the laser spot illuminates a region of area $A = 100\ \mu\text{m}^2$. The absorption depth of the substrate has been ignored, so the results only apply to a subsurface defect very close to the surface. Some of the signal from a defect or a particle is reduced by the addition of polarizers, however to a lesser degree than that for microroughness.

The intersection of the scatter curves from each mechanism yields an estimate of the particle or defect radius that can be detected above the noise of the microroughness-induced scatter. It can be seen from Fig. 4 that the use of the detection scheme shown in Fig. 3 should yield a factor of about 1.4 improvement in the detectable particle or defect radius. Further improvements can be made by making use of the different scattering sources' intensity distributions in addition to their polarizations, that is, by only collecting over select solid angles.

SUMMARY

It has been found that the polarization of light scattered by a surface can reveal the source of scattered light. Results of measurements of the polarization of light scattered by roughness were compared to those of theoretical models, and the agreement is very good. To demonstrate the utility of polarized light scatter techniques, the predicted performance of a particular device was calculated, yielding a factor of approximately 1.4 improvement in the radius of a detectable particle or defect. Although specific designs may yield different levels of improvement, it is expected that these techniques will extend the capabilities of light scattering tools for the inspection of silicon wafers.

ACKNOWLEDGMENTS

The author would like to thank Bradley Scheer of VLSI Standards, Inc., for supplying the microrough silicon samples, and Clara Asmail for many useful discussions.

REFERENCES

1. Germer, T. A., Appl. Opt. **36**, 8798–8805 (1997).
2. Germer, T. A., and Asmail, C. C., Proc. SPIE **3121**, 173–82 (1997).
3. Germer, T. A., Asmail, C. C., and Scheer, B.W., Opt. Lett. **22**, 1284–6 (1997).
4. Germer, T. A., and Asmail, C. C., Provisional U.S. Patent Application Filed (1997).
5. Barrick, D. E., *Radar Cross Section Handbook* (Plenum, New York, 1970).
6. Elson, J. M., J. Opt. Soc. Am. **66**, 682–94 (1976); Appl. Opt. **16**, 2873-81 (1977); J. Opt. Soc. Am. **69**, 48–54 (1979); J. Opt. Soc. Am. A **12**, 729–42 (1995).
7. Germer, T. A., Proc. SPIE **3275**, in press (1998).
8. Kröger, E. and Kretschmann, E., Z. Physik **237**, 1 (1970).
9. Germer, T. A., and Asmail, C. C., Proc. SPIE **3141**, 220–31 (1997).
10. Bender, H., Vanhellemont, J., Schmolke, R., Jpn. J. Appl. Phys. Part 2 **36**, L1217–20 (1997).
11. Germer, T. A., and Asmail, C. C., Proc. SPIE **2862**, 12–7 (1996).